Christopher Lockhart and Dmitri K. Klimov
"Molecular interactions of Alzheimer's biomarker FDDNP with Aβ peptide"

Supporting Materials

Parameterization of FDDNP molecule: CHARMM General Force Field (CGenFF version 2b6) was used to generate the parameters for FDDNP molecule [1]. CGenFF implemented through the ParamChem web interface produced FDDNP force field parameters using existing parameterizations of analogous chemical structures. FDDNP atom charges were adjusted to keep the net charge of the compound as zero. The mass of aliphatic monofluoro atom was manually changed to account for the mass of ^{18}F isotope. CHARMM MD program compiled with CGenFF was then used to identify the missing parameters and energetically minimize the final molecular structure.

Convergence of REMD simulations: The convergence of REMD sampling was tested using several methods described in our previous studies ([2] and ref. [40] in the main text). Below we evaluate REMD convergence for the system consisting of Aβ monomer and 10 FDDNP ligands (system S1), although similar results were obtained for the system containing three ligands (system S2). First, we have computed the number N_s of unique states (E_p,C) sampled at least once in the course of simulations. Each state (E_p,C) is determined by the potential energy E_p and the number of intrapeptide side chain contacts, C. The energy interval used to discretize potential energies is 2 *kcal/mol,* whereas the full range of E_p is approximately 10,000 *kcal/mol*. The number N_s as a function of the cumulative equilibrium simulation time τ_{sim} is shown in Fig. S1. It is seen that N_s starts to level off at τ_{sim} >1.0 μs indicating that REMD sampling gradually exhausts new states. To test the convergence of sampling of ligand binding, we have considered the states (E_p,L), where L is the number of bound ligands. The number of unique states (E_p,L) indicate that REMD simulations start to revisit already sampled states at τ_{sim} >0.6 μs. Exhaustion of the new states observed for two independent quantities probing peptide conformational ensemble and ligand binding suggests the convergence of REMD simulations.

To perform the second test of REMD convergence we computed the replica mixing parameter *m(T)* introduced by Han and Hansmann [3]

$$m(T) = 1 - \frac{\sqrt{\sum_i t_i^2}}{\sum_i t_i},$$

where t_i is the total number of REMD steps spent by the replica i at the REMD temperature T. If the total number of replicas is N=40 and all replicas are equally represented at the temperature T, $m(T) = 1 - 1/\sqrt{N} \approx 0.84$. Then if constant *m(T)*≈0.84 is observed for *all* REMD temperatures, it would indicate efficient mixing of replicas over temperatures and no evidence of their trapping at any temperature. Fig. S2 shows that *m(T)* is indeed approximately constant and equal to ≈0.8 for all REMD temperatures.

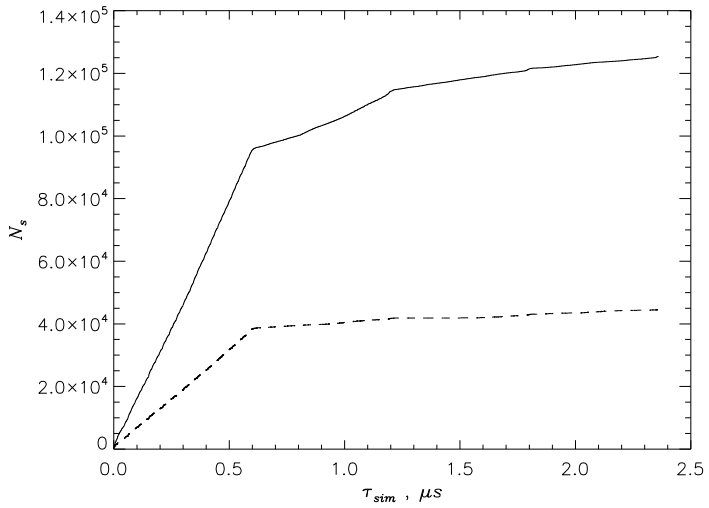

Fig. S1 The number N_s of the unique states (E_p,C) as a function of the cumulative equilibrium simulation time τ_{sim} (continuous line). Dotted line represents N_s computed for the states (E_p,L). Data are for the system S1.

Mixing of replicas over temperatures is directly visualized in Fig. S3. This figure demonstrates random walk of replicas over temperatures as prescribed by REMD. Finally, we checked REMD convergence by dividing the simulation data into two equal subsets and analyzing them separately. The thermodynamic quantities probing Aβ monomer structure from the two subsets differed by no more than 4% at 330K. The errors in the quantities describing ligand-peptide interactions did not exceed 16%. Corresponding errors for the system containing three FDDNP ligands were within 10 and 17%.

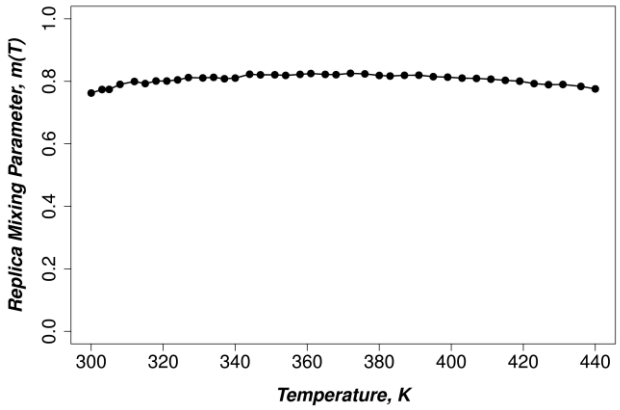

Fig. S2 Replica mixing parameter *m(T)* as a function of REMD temperatures *T*.

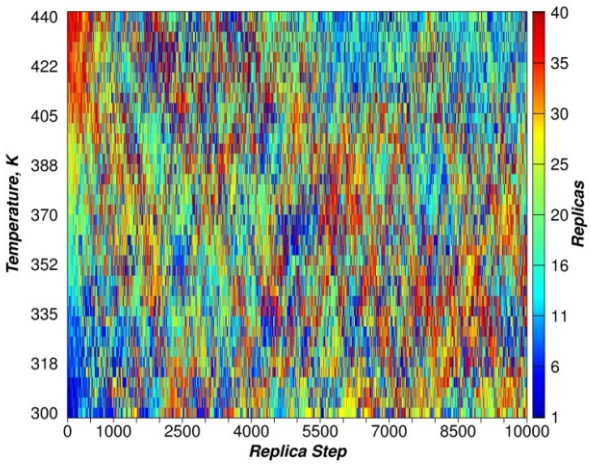

Fig. S3 Random walk of replicas over temperatures in REMD trajectory for the system S1. Colors in the right scale represent instantaneous distribution of replicas over temperatures at the beginning of the REMD trajectory.

Changes in polar accessible surface areas of amino acids and FDDNP binding: We have computed changes in the relative polar accessible surface areas (ASA) $<\delta pASA(i)>$ of amino acids *i* caused by ligand binding. Fig. S4 shows $<\delta pASA(i)>$ together with the number of ligand-amino acid contacts $<C_l(i)>$. Lack of correlation between $<\delta pASA(i)>$ and $<C_l(i)>$ indicates that the interactions with polar atoms do not play a significant role in FDDNP binding.

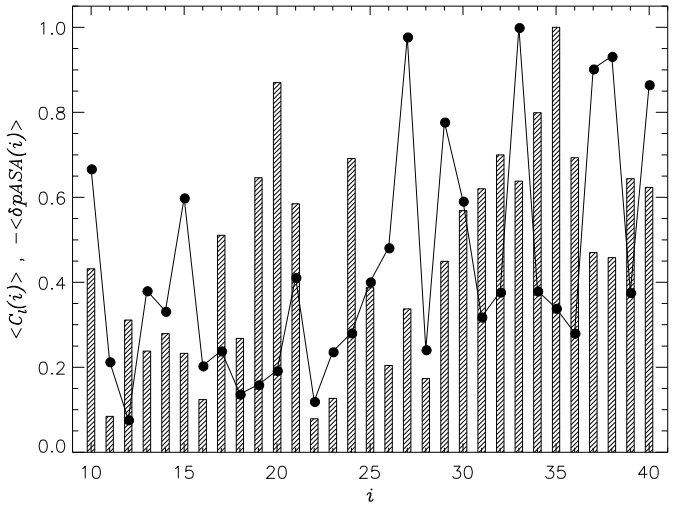

Fig. S4 The plot compares changes in the relative polar ASA $<\delta pASA(i)>$ of amino acids *i* (black circles) with the numbers of contacts formed by Aβ side chains *i* with FDDNP ligands, $<C_l(i)>$ (shaded bars). The plot is computed at 330K for high ligand concentration.

FDDNP molecules penetrate the core of Aβ peptide: To explore the spatial distribution of FDDNP ligands around Aβ we computed the number densities for various atoms *g(r)* as a function of the distance to Aβ center of mass *r*. Fig. S5 shows that the number density of peptide atoms $g_p(r)$ rapidly decays reaching half of its $g_p(0)$ value at $r=R_c$ (=10Å), which we interpret as the boundary of Aβ core. Our computations indicate that about 59% of hydrophobic amino acids are confined to the core. The ligand number density $g_l(r)$ also presented in Fig. S5 indicates that some ligands penetrate Aβ core. Indeed, it follows from Fig. S5 that 23% of ligand atoms are localized in the core. Therefore, although most of FDDNP ligands concentrate around Aβ core (the inset to Fig. S5), a noticeable fraction resides inside its core. This result can be expected, because Aβ core contains large fraction of hydrophobic atoms and FDDNP binding is mainly governed by hydrophobic effect.

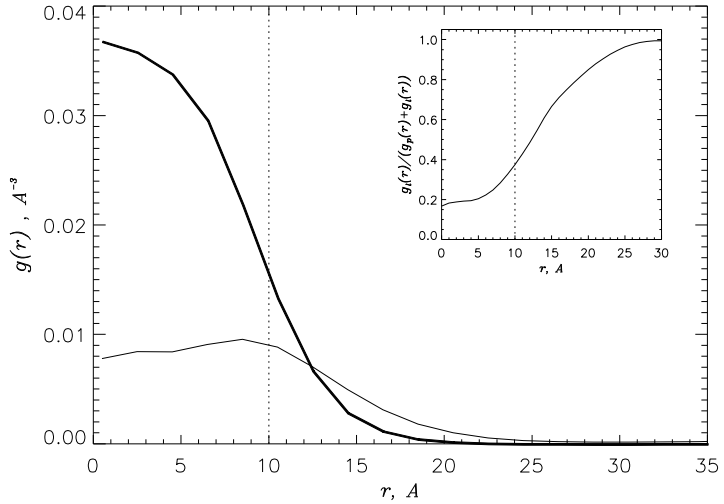

Fig. S5 Number density of Aβ atoms $g_p(r)$ as a function of the distance to Aβ center of mass *r* (thick black line). Number density of FDDNP atoms $g_l(r)$ is given by thin line. The inset presents the fraction of ligand atoms $g_l(r)/(g_l(r)+g_p(r))$ vs *r*. Dashed vertical lines indicate the boundary of Aβ core. The figure is obtained for high ligand concentration at 330K.

Rigidity of Aβ backbone is affected by R1-R2 intrapeptide interactions: Formation of R1-R2 interactions significantly enhances the rigidity of Aβ backbone. As an illustration consider Fig. S6, which displays two distributions of standard deviations of backbone dihedral angles, $\delta\phi(i)$ and $\delta\psi(i)$, computed for the cases when R1-R2 interactions are formed or broken. If R1-R2 interactions are formed (i.e., at least one contact in bold in Table 2 is established), the average of $\delta\phi$ and $\delta\psi$ in the sequence region (15-24) is $36(\pm5)^\circ$. However, if R1-R2 interactions are broken, this average increases to $48(\pm1)^\circ$. The sequence region with the stiff backbone (15-24) approximately coincides with the region of elevated turn content in Fig. 4a.

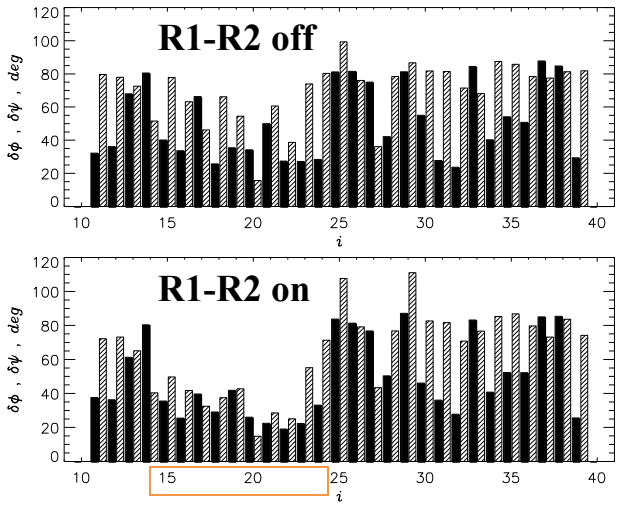

Fig. S6 Distributions of fluctuations in Aβ backbone measured by the standard deviations in backbone dihedral angles $\delta\phi(i)$ (filled bars) and $\delta\psi(i)$ (shaded bars) as a function of sequence position i. The lower and upper panels are computed with R1-R2 interactions formed or disrupted. The list of R1-R2 interactions is given in bold in Table 2. The sequence region with stiff backbone is boxed in the lower panel. The plots are obtained for high ligand concentration at 330K.

Tertiary structure of Aβ monomer in ligand free water: To evaluate the changes in Aβ tertiary structure induced by FDDNP we have computed the map of contacts $<C(i,j)>$ between Aβ side chains i and j in ligand free water (Fig. S7). This figure shows numerous local interactions ($|j-i|<5$) and few long range contacts formed between the residues near the central hydrophobic cluster (Phe19, Val24) and in the C-terminal (Gly29, Ileu31, Val34, Met35). The distribution of long range (tertiary) intrapeptide interactions in ligand free water is sharply different from those observed at low or high FDDNP concentrations (Figs. 4b and 5c).

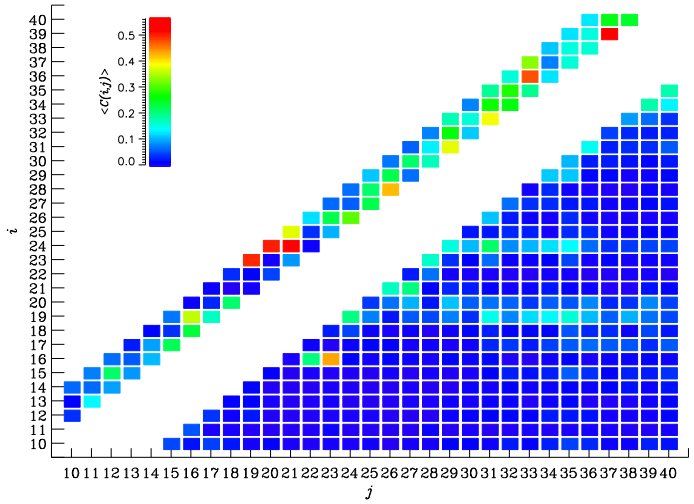

Fig. S7 Contact map $<C(i,j)>$ visualizes the probabilities of forming side chain contacts between residues i and j in ligand free water at 330K ($i<j$). The map is computed using REMD sampling of Aβ10-40 monomer (ref. [40] in the main text). Local contacts ($|j-i|<5$) are shown above the main diagonal, i.e., for those $j<i$.

Testing the secondary structure distribution in Aβ peptide: Using STRIDE program we have shown that FDDNP binding does not change significantly the secondary structure of Aβ peptide. To test this conclusion we have applied another commonly used program for secondary structure analysis, DSSP (ref. [48] in the main text). Fig. S8 compares the fractions of helix <*h(i)*>, turn <*t(i)*>, bend <*s(i)*>, and random coil <*rc(i)*> formed by residues *i* at high FDDNP concentration and in ligand free water. It is clear that apart from the sequence region around Gln15 the distributions are similar. The average fractions of helix structure <*h*> in S1 and ligand free water are ≈0.11 and ≈0.13, respectively. For turn <*t*>, random coil <*rc*>, and bend <*s*> fractions the corresponding approximate values are 0.25 and 0.23, 0.41 and 0.44, 0.21 and 0.19. Hence, DSSP predicts minor redistribution of secondary structure with some increase in bend propensity near Gln15. Note that STRIDE, which does not distinguish bend, predicts enhancement of turn structure in the same region (Fig. 4a). With respect to ligand free water the RMSD values for the helix, turn, random coil, and bend structures formed by individual amino acids are 0.05, 0.07, 0.14, and 0.10, which are similar to those computed using STRIDE. Therefore, DSSP and STRIDE suggest that FDDNP binding causes minor changes in Aβ secondary structure.

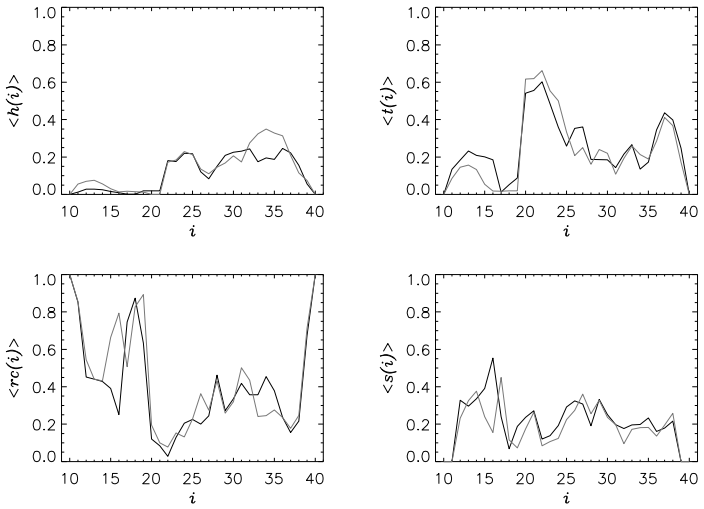

Fig. S8 Distributions of Aβ secondary structure computed using DSSP at 330K: fractions of helix <*h(i)*>, turn <*t(i)*>, bend <*s(i)*> , and random coil <*rc(i)*> structures formed by Aβ residues *i* in high FDDNP concentration solution and in ligand free water are shown in black and grey, respectively.

Supporting references

1. Vanommeslaeghe, K., Hatcher, E., Acharya, C., Kundu, S., Zhong, S., Shim, J., Darian, E., Guvench, O., Lopes, P., Vorobyov, I., and MacKerell, A. D., 2009. CHARMM general force field: A force field for drug-like molecules compatible with the CHARMM all-atom additive biological force fields. *J. Comp. Chem.* 31: 671–690.
2. Kim, S., Takeda, T., and Klimov, D.K., 2010. Globular state in the oligomers formed by Abeta peptides *J. Chem. Phys.* 132:225101.

3. Han, M., and Hansmann, U. H. E., 2011. Replica exchange molecular dynamics of the thermodynamics of fibril growth of Alzheimer's Aβ42 peptide. *J. Chem. Phys.* 135:065101.